

Enhancing Nuclear Resonance Fluorescence with Coded Aperture for Security Based Imaging

Zachary Sun, W. Clem Karl, David Castañón

Abstract

Nuclear resonance fluorescence (NRF) is a nuclear phenomenon where the nucleus can be made to emit a spectral pattern that can be used to distinguish the material. This effect is triggered by exposing the material to a continuous spectrum of high-energy photons and then observing the resulting fluorescence spectrum, which varies with material. The photons used in the excitation process occur at energy levels of 2-8 MeV, which are among the most penetrating and can see through several inches of steel. The combination of material specific signatures and high penetration are well matched to applications such as cargo screening for threats and contraband. An imaging system has been proposed based on NRF using straight forward raster scanning of an excitation beam combined with simple collimation of the resulting emissions. While such a system is computationally inexpensive, it results in low inherent signal-to-noise ratio because most emitted photons are discarded, necessitating long scanning times. In this work we propose and explore the use of a coded aperture to increase the signal-to-noise ratio and lower acquisition time of NRF-based imaging.

Introduction

From the physical properties of materials it follows that for nearly every nuclei of atomic number $Z > 2$, there exists states of excitation that can be initiated by photon absorption that subsequently decay by emission of photons. These emissions create a unique emission spectrum for the corresponding nuclear isotope [1, 2] which could be used to classify or separate materials. As an example, Figure 1 shows the corresponding such spectra for three different materials. To produce these spectra a material is excited by an X-ray beam in the 2-8MeV range. Both the excitation as well as the emission of photons in different energy bands do not interact and be assumed independent of each other. As a result the overall problem can be treated as a series of independent estimations for each energy band.

Beams in the 2-8MeV excitation energy range are quite penetrating, able to pass through several inches of steel. This combination of good material penetration and material specific signature makes NRF potentially attractive for the detection and classification of threats and contraband in cargo and transported goods.

Localization through Collimation

To be useful for security and policing applications a method of spatial localization is needed. An imaging system has been proposed based on NRF using straight forward raster scanning of a 2-8 MeV excitation beam combined with simple collimation of the resulting emissions. The beam is scanned through objects of interest and then the emitted photon spectrum from the decaying states is collected via photon-counting detectors preceded by par-

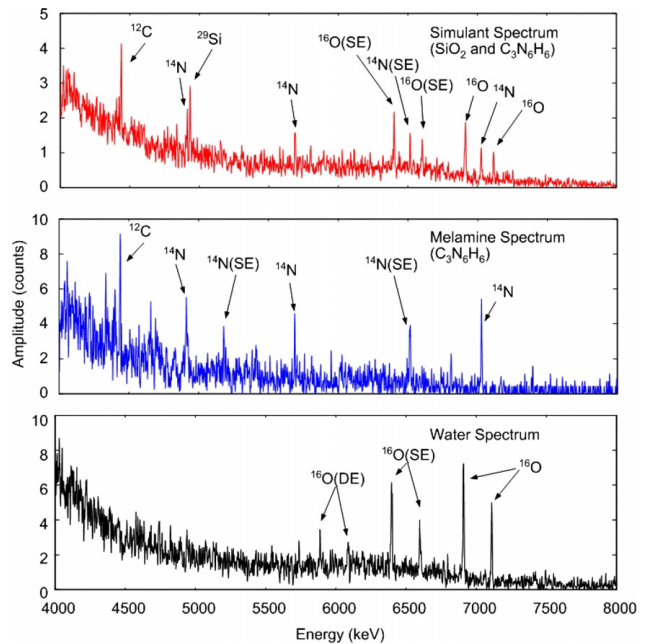


Figure 1. Example Nuclear Resonance Fluorescence Spectral Output [1]

allel collimators, which localize the emission to a line of response in space. The intersection between the collimated detector line of response and the illuminating source beam defines a localized material pixel. Figure 2 shows an example setup for one position of the illuminating beam. Unfortunately, the use of collimation means that a significant portion of the emitted photons are not collected, resulting in measurement system that is photon inefficient. Consequently, acquisition times of 20-30 minutes are needed to produce reasonable SNR levels and readouts such as Figure 1 for a single excitation line. The result is that entire volumes cannot be tractably scanned. Instead, areas of interest are first identified via an initial tomographic scan, then collimated source and detectors are focused on the area of interest to acquire sufficient photons and SNR to make a material determination.

Proposed Coded Aperture Approach

In an effort to improve the number of photons detected, and thus increase SNR and reduce acquisition time, we propose to replace the current collimation based localization with a coded aperture approach [3]. A raster-based excitation is still used, wherein each row of a scene $X(i)$ is still individually illuminated. But instead of using collimation for additional localization, and in the process discarding a large majority of the emitted photons, we propose to use a coded mask, thus capturing many more of the

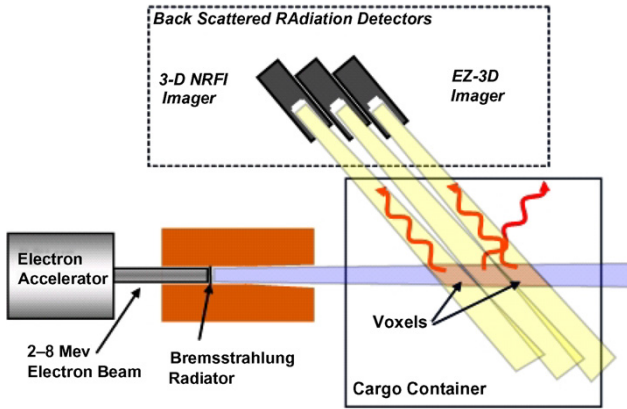


Figure 2. Diagram of a NRF system from Passport Systems, Inc. A single row of a container is illuminated and then collimated detectors observe fixed positions along the path of illumination. [1]

emitted photons. Each detector now sees a coded version of the emitted photon distribution, and this coding then needs to be modeled and inverted. We assume that photons that illuminate the material and photons that are emitted are attenuated according to Beer's law and thus the absorption characteristics reduce the number of photons observed. Since each energy band is independent we focus on estimating and localization of emission in a single energy band. The governing model for this energy band then becomes:

$$\mathbf{I}_{\text{coded}}(i) = \mathbf{Y}_{\text{coded}}(i) + n(i), \quad i = 1, 2, \dots, N \quad (1)$$

where $\mathbf{I}_{\text{coded}}(i)$ is the data acquired while illuminating row i , $\mathbf{Y}_{\text{coded}}(i)$ is the amount of photons produced by the material being that imping on the detectors, $n(i)$ is readout noise, and N is the number of rows to be scanned. The number of material generated photons at the detector $\{\mathbf{Y}_{\text{coded}}(i), i = 1, 2, \dots, N\}$ form a Poisson process with a mean value $\{\mu_{\text{coded}}(i), i = 1, 2, \dots, N\}$ where

$$\mu_{\text{coded}}(i) = h_i * \mathbf{X}(i), \quad i = 1, 2, \dots, N \quad (2)$$

such that $\mathbf{X}(i)$ is the corresponding distribution of material fluorescence in the row being illuminated and h_i captures the overall influence of the observation system. This convolutional kernel includes the effect of both the coded mask we are using as well as the aggregate effects of an attenuation from surrounding material and will thus vary from row to row. We assume the attenuation characteristics are known a priori due to a previously computed tomographic image. Overall, the collection of observations for each illuminated row forms a linear system of equations (Eq. 3) such that H is block diagonal where each block is the 1-D convolutional matrix for row i .

$$\mu_{\text{coded}} = H\mathbf{X} \quad (3)$$

The dominant statistics are assumed to arise from the Poisson term, thus for reconstruction purposes we assume that the readout noise component can be ignored and that $\mathbf{I}_{\text{coded}}$ is distributed as

$$p(\mathbf{I}_{\text{coded}}|\mathbf{X}) = \frac{(H\mathbf{X})^{\mathbf{I}_{\text{coded}}} e^{-(H\mathbf{X})}}{\mathbf{I}_{\text{coded}}!} \quad (4)$$

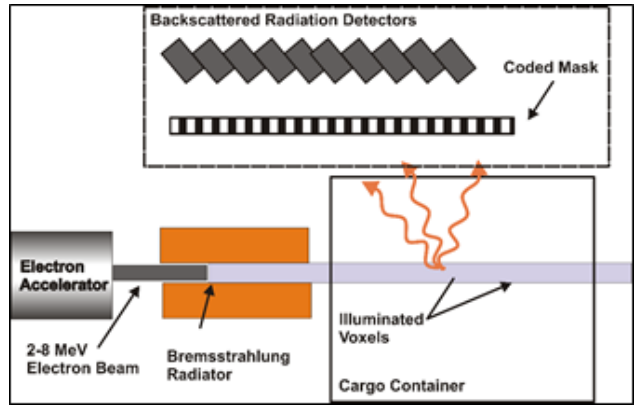


Figure 3. Our proposed approach to replace the collimators with a coded aperture allowing a higher photon capture rate from angles that collimators discard.

We generate an emission estimate from the coded observations by solving an optimization problem derived from the negative log likelihood (Eq. 5) of the data combined with a derivative penalty $\|D\mathbf{X}\|_2^2$ weighted by a regularization parameter α .

$$\hat{\mathbf{X}} = \underset{x}{\text{argmin}} -\log(p(\mathbf{I}_{\text{coded}}|\mathbf{X})) + \alpha\|D\mathbf{X}\|_2^2 \quad (5)$$

Substituting in Eq. 4 we minimize the penalized poisson negative log likelihood function (Eq. 6) with a non-negativity constraint.

$$\hat{\mathbf{X}} = \underset{x}{\text{argmin}} H\mathbf{X} - \mathbf{I}_{\text{coded}} \log(H\mathbf{X}) + \alpha\|D\mathbf{X}\|_2^2 \quad (6)$$

Variety of algorithms are commercially available to solve Eq. 6 such as trust region methods[5] or interior point methods[6].

Preliminary Experimental Results

For our preliminary simulations, we assume that each energy band is independent of each other and can be separately reconstructed; therefore, we focus on a monochromatic problem for a single energy band. We constructed a 256cm square phantom for one energy band to simulate a cargo container with boxes lined with dense, fluorescent material (Figure 4). Being a monochromatic phantom, each pixel in Figure 4 would be one scalar value of a spectral plot similar to Figure 1.

Material	Total Attenuation (cm^{-1})	Fluorescent Rate (# of photons)
Material 1	0.01	4
Material 2	0.012	5
Material 3	0.015	7
Material 4	0.02	10
Water	0.022	12
Graphite	0.03	15
Aluminum Box	0.07	20

Table 1: Material Absorption Characteristics with Arbitrary Fluorescent Values

Source illumination was simulated from the left as shown with Figures 2 and 3. Absorption numbers were taken from the NIST

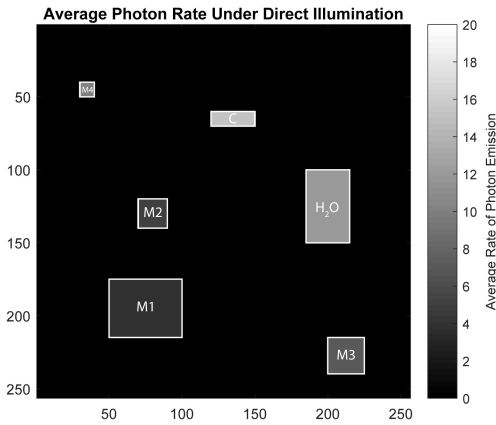


Figure 4. A 256cm x 256cm Simulated Phantom at a single energy band, X. Boxes of homogeneous material of various fluorescence and absorption characteristics are placed inside 1cm thick high fluorescent dense material.

XCOM: Photon Cross Sections Database to simulate aluminum boxes with various common organic material. The fluorescent values were chosen more arbitrarily (Table 1).

We simulate the forward model in both collimated and coded case using the convolution forward model (Eq. 1). The collimated forward model simplifies Eq. 1 where the mean value function in the Poisson term is replaced with Eq. 7. A diagonal forward operator (W) with weights based on the absorption properties of the direct ray paths from source to excitation and then emission to detector replaces the coded mask operator (H).

$$\mu_{\text{collimated}} = WX \quad (7)$$

Our proposed coded mask (Figure 5) was simulated using a random mask with 50% throughput of the same width as the image which we position equidistant between the top of the image and



Figure 5. A 256cm wide Coded Random Mask, h , with 50% throughput.

the detectors, as described with Figure 6.

We simulate the forward model by individually computing each ray trace from source to excitation pixel and then from emission source to detector using Siddon's method [4] and taking into account path attenuation. Figure 7a is what the current collimated system would see if the entire image were to be scanned. Depending on the object's position within the image, certain areas have higher photon starvation than others, with the worst offenders being some of the aluminum edges in the bottom right box (furthest from both the detectors and the illuminating source). Figure 7b is our proposed coded approach where there is a large increase in photons detected at the cost of coded localization information.

We then solve Eq. 5 for both the collimated and coded case with a non-zero constraint using MATLAB's interior point method[6]. Parameter α was selected by searching for the minimum reconstruction mean squared error. The reconstruction of the coded image (Figure 8b) came through brighter with more defined edges and a lower MSE by nearly a factor of 3 over the attenuation corrected collimated image (Figure 8b).

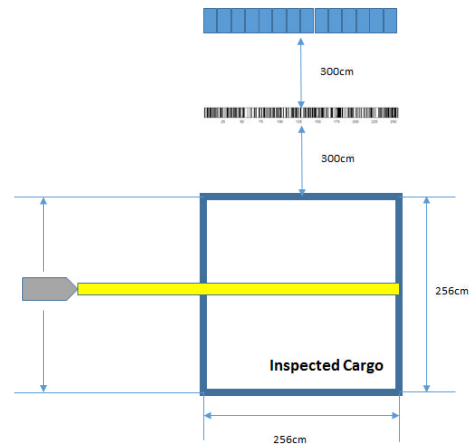


Figure 6. Our simulated setup's geometry The coded mask is positioned equidistant from the sensor to the top of the image along with source illumination from the left. The source is then swept along each row to generate an image of equivalent size.

Conclusions and Future Work

Our current approach by applying a coded mask increases the number of photons that arrive at the detectors. Potentially this can lower the acquisition time needed to have sufficiently high data SNR.

The simulations in this work were for a single energy band, as we assumed all energy bands were independent of each other. Some form of joint reconstruction across the spectrum could yield improved reconstruction results that are more consistent with material spectral signatures. In addition, alterations in geometry such as mask distances, type of masks, and mask size are all areas to explore for improving reconstruction results.

Acknowledgments

This material is based upon work supported by the U.S. Department of Homeland Security, Science and Technology Directorate, Office of University Programs, under Grant Award 2013-ST-061-ED0001. The views and conclusions contained in this document are those of the authors and should not be interpreted as necessarily representing the official policies, either expressed or implied, of the U.S. Department of Homeland Security.

References

- [1] William Bertozzi, Stephen E. Korbly, Robert J. Ledoux, William Park, Nuclear resonance fluorescence and effective Z determination applied to detection and imaging of special nuclear material, explosives, toxic substances and contraband, Nuclear Instruments and Methods in Physics Research Section B: Beam Interactions with Materials and Atoms, Volume 261, Issues 1–2, August 2007, Pages 331–336, ISSN 0168-583X
- [2] William Bertozzi, Robert J. Ledoux, Nuclear resonance fluorescence imaging in non-intrusive cargo inspection, Nuclear Instruments and Methods in Physics Research Section B: Beam Interactions with Materials and Atoms, Volume 241, Issues 1–4, December 2005, Pages 820–825, ISSN 0168-583X
- [3] Scott T. McCain ; B. D. Guenther ; David J. Brady ; Kalyani Krishnamurthy ; Rebecca Willett; Coded-aperture Raman imaging for standoff explosive detection. Proc. SPIE 8358, Chemical, Biologi-

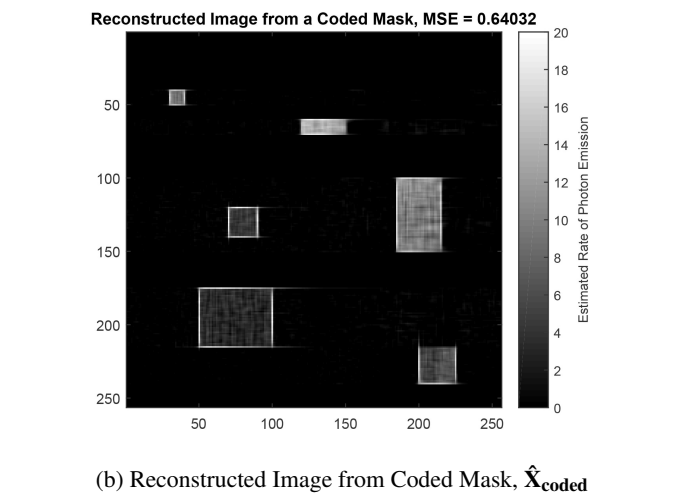
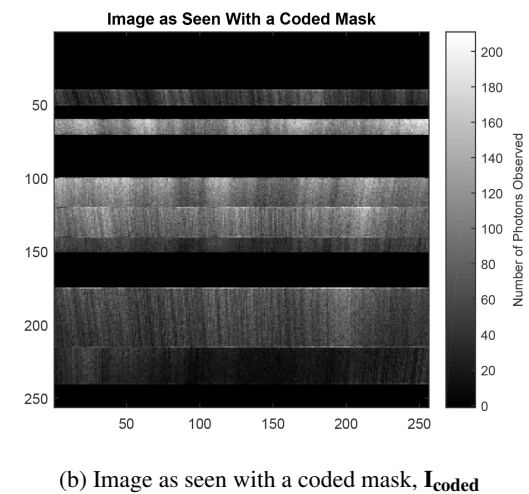
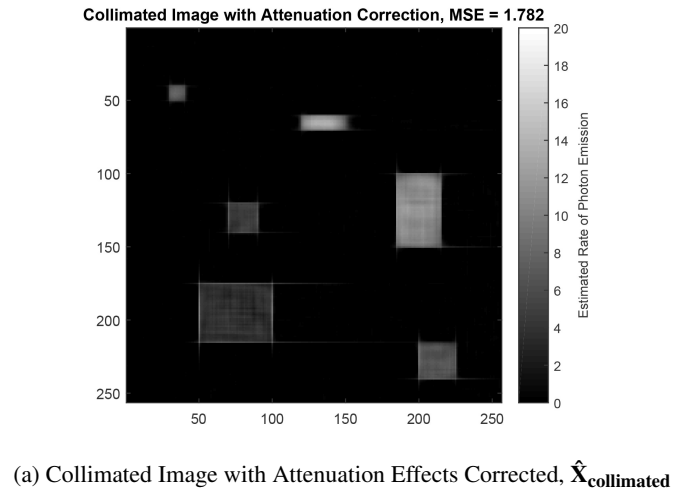
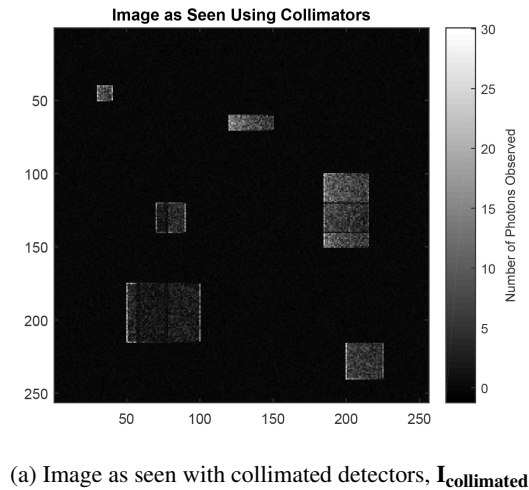


Figure 7. (a) A simulated image of what collimated detectors would observe at each pixel. Absorption of other materials in the pathway create areas dimmer than the rest depending on obscuration (b) Image as seen with a 50% throughput coded mask allowing higher photon counts at the loss of localization.

Figure 8. (a) Correcting for attenuation effects with a smoothness penalty results in a dimmer image than was observed with less pronounced edges. (b) Deconvolution of the coded mask recovers an image that is brighter with sharper edges and lower MSE.

cal, Radiological, Nuclear, and Explosives (CBRNE) Sensing XIII, 83580Q (May 1, 2012)

- [4] Robert L. Siddon, Fast calculation of the exact radiological path for a three-dimensional CT array, *Medical Physics*, 12, 252-255 (1985)
- [5] Richard H. Byrd, J. C. Gilbert, and J. Nocedal. "A Trust Region Method Based on Interior Point Techniques for Nonlinear Programming." *Mathematical Programming*, Vol 89, No. 1, 2000, pp. 149–185.
- [6] Richard H. Byrd, Mary E. Hribar, and Jorge Nocedal. "An Interior Point Algorithm for Large-Scale Nonlinear Programming." *SIAM Journal on Optimization*, Vol 9, No. 4, 1999, pp. 877–900.

Author Biography

Zachary Sun received his BS in Electrical Engineering from Tufts University (2008) and is currently working towards completing his PhD in Electrical Engineering at Boston University. His work has been a part of the Department of Homeland Security's Awareness and Localization of Explosives-Related Threats (ALERT) Center of Excellence. His re-

search interests include tomographic imaging, machine learning, and inverse problems.

W. Clem Karl received the Ph.D. degree in Electrical Engineering and Computer Science from the Massachusetts Institute of Technology. He is currently Professor of Electrical and Computer Engineering and Biomedical Engineering at Boston University. Dr. Karl's research interests are in the areas of computational imaging, statistical signal and image processing, estimation, detection, and medical signal and image processing. He has served as the Editor-in-Chief of the *IEEE Transactions on Image Processing* and is currently the inaugural Editor-in-Chief of the *IEEE Transactions on Computational Imaging*.

David Castañón received his PhD in Applied Mathematics from MIT (1976). He was Chief Scientist at ALPHATECH, Inc. before joining Boston University in 1990 where he serves as Professor of Electrical and Computer Engineering. His research interests include stochastic control, estimation, game theory, optimization, and inverse problems. He is Associate Director of the ALERT Center of Excellence on Explosives Detection and Mitigation.